Supporting Information

Deterministic Absolute Negative Mobility for Micro- and Submicrometer Particles Induced in a Microfluidic Device

Jinghui Luo,[†,⊥] Katherine A. Muratore,[‡] Edgar A. Arriaga,[‡,§] and Alexandra Ros[*,†,⊥]

[†]School of Molecular Sciences, and [⊥]Center for Applied Structural Discovery, The Biodesign Institute, Arizona State University, Tempe, Arizona 85287, United States
[‡]Department of Biochemistry, Molecular Biology and Biophysics, and [§]Department of Chemistry, University of Minnesota, Minneapolis, Minnesota 55455, United States

*Corresponding author. E-mail: alexandra.ros@asu.edu. Phone: +1-480-965-5323. Fax: +1-480-965-7954.

This material contains the supplementary theory and equations for the numerical modeling, the electrokinetic mobility measurement for 4.4-μm polystyrene beads, a supplementary figure showing the migration velocity obtained from the refined simulation for 4.4 μm particles, and the information on the supplementary videos.

1. Supplementary Theory and Equations for Numerical Modeling

When an electric field, $\boldsymbol{E}$, is applied to a microfluidic channel (Figure 1a) containing an aqueous suspension of negatively-charged particles, a positive electroosmotic flow (EOF) and electrophoresis (EP) of the particle induce the apparent velocity $\boldsymbol{u}$:

$$\boldsymbol{u} = \mu_{ek}\boldsymbol{E} = (\mu_{eo} - \mu_{ep})\boldsymbol{E} \qquad (\mathrm{S}-1)$$

where μ_{ek}, μ_{eo}, and μ_{ep} represent the electrokinetic mobility, EOF mobility and EP mobility, respectively. In order to induce DEP as an additional migration effect, a system is constructed containing obstacles, such as the non-linear array of insulating posts in a microfluidic channel shown in Figure 1b. Electric field gradients are created around the insulating posts due to the application of potentials in the microchannel reservoirs. The arising DEP force on a spherical particle can be expressed as:[1-4]

$$\boldsymbol{F}_{dep} = 2\pi R^3 \varepsilon_m f_{\mathrm{CM}} \nabla \boldsymbol{E}^2 \qquad (\mathrm{S}-2)$$

where R is the particle radius and ε_m is the medium permittivity:

$$\varepsilon_m = \varepsilon_{r,m}\varepsilon_0 \qquad (\mathrm{S}-3)$$

where $\varepsilon_{r,m}$ is the relative permittivity of the medium (80 for water[5]) and ε_0 is the vacuum permittivity. The Clausius-Mossoti factor f_{CM} under DC and low frequency conditions is calculated by:[1-3]

$$f_{CM} = \frac{\sigma_p - \sigma_m}{\sigma_p + 2\sigma_m} \qquad (\mathrm{S}-4)$$

where σ_p and σ_m are the conductivity of the particle and the medium, respectively. The value of f_{CM} used in the preliminary simulation is estimated to be -0.5 based on the literature value of σ_p for polystyrene[6, 7] and σ_m measured in the employed solution (0.03 S/m). For the parameter sweep of the DEP mobility used in the refined simulation, the f_{CM} value varied from -0.08 to -0.4 corresponding to μ_{dep} from -1 to -5 $\times 10^{-19}$ $m^4 \cdot V^{-2} \cdot s^{-1}$.

The contribution of the DEP force to the migration of a particle can be expressed by the DEP velocity $\boldsymbol{v}_{dep}$:[3]

$$\boldsymbol{v}_{dep} = \mu_{dep}\nabla \boldsymbol{E}^2 = \frac{R^2 f_{CM}\, \varepsilon_m}{3\eta}\nabla \boldsymbol{E}^2 \qquad (\mathrm{S}-5)$$

where η is the viscosity of the medium. We have performed a COMSOL simulation to compare the migration velocity of particles suspended in an aqueous solution (viscosity = 8.90×10^{-4} Pa·s for water at 25 °C) to that suspended in a sucrose solution (1.3× water viscosity) with similar parameters as used in our study. The results revealed that the velocities obtained at the two viscosities were statistically the same at 95% confidence interval (data not shown). Therefore, the viscosity of water at 25 °C was used in all the simulations.

Based on the Stokes drag law, the drag force ($\boldsymbol{F}_d$) is given as:[3]

$$\boldsymbol{F}_d = 6\pi\eta R(\boldsymbol{u} - \boldsymbol{v}) \qquad (\mathrm{S}-6)$$

where $\boldsymbol{u}$ is the fluid velocity and $\boldsymbol{v}$ is the particle velocity. Newton's second law can be utilized to solve for the instant velocity of the particle:

$$\frac{d(m_p \boldsymbol{v})}{dt} = \boldsymbol{F}_t \qquad (\mathrm{S}-7)$$

where m_p is the particle mass and $\boldsymbol{F}_t$ stands for the total force applied on the particle at time t. This equation is used in the numerical modeling to calculate and visualize the particle trajectory, as shown in the main manuscript.

2. Electrokinetic mobility measurement for 4.4-µm polystyrene beads

The chip and bead solution preparation were similar to the procedures for dANM experiments as described in the main manuscript. The experiment was however performed using a straight channel without posts. Beads were introduced into the channel by capillary action, the liquid level was well balanced and subsequently a DC signal was supplied by the high voltage amplifier. The

resulting bead migration was recorded with a video camera as described in the main manuscript. The migration of beads was imaged at 20, 40, 60, 80 and 100 V/cm. Over 100 individual trajectories for 4.4-µm beads at each DC voltage were analyzed by MTrack2 plugin (see reference (36) in the main manuscript) to obtain migration distances over defined time intervals. After plotting the average migration velocity versus the applied DC electric field, the electrokinetic mobility of 4.4-µm beads was obtained by calculating the slope of the least squares line, which resulted in 2.2×10^{-9} $m^2 \cdot V^{-1} \cdot s^{-1}$ ($R^2 = 0.9946$). This value was used in the refined simulations.

3. Supplementary figure

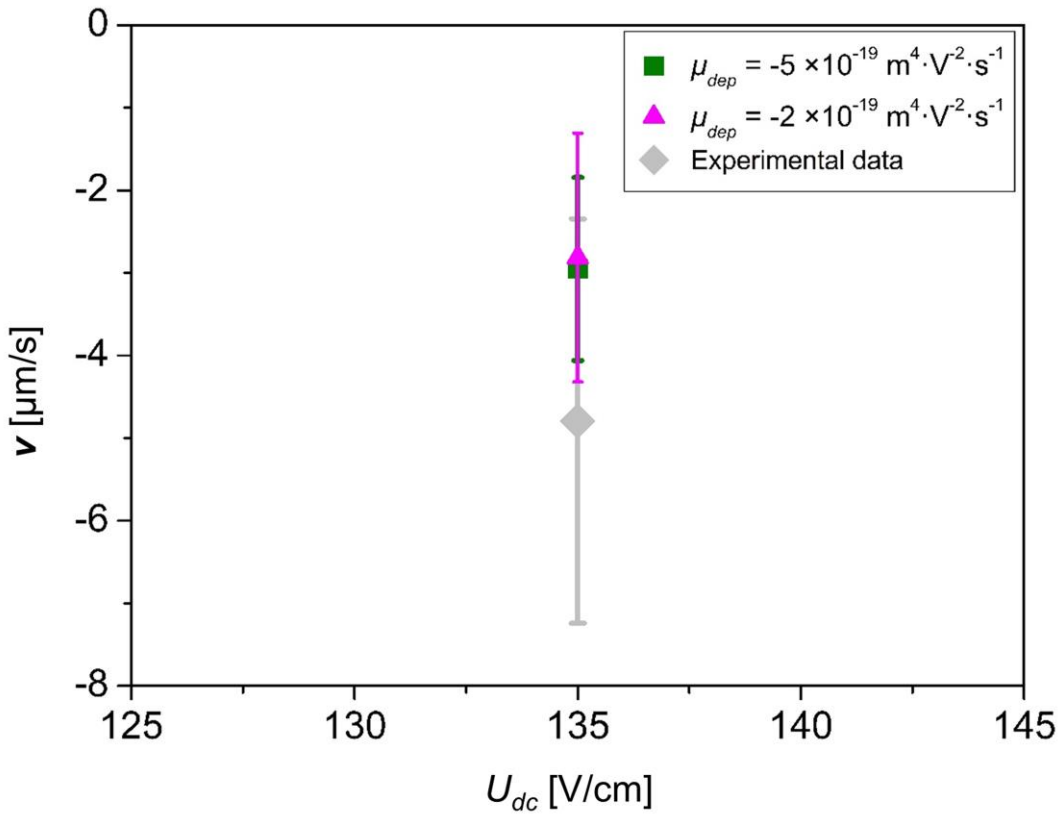

Figure S-1: Migration velocity obtained from the refined simulation for 4.4 µm particles at U_{ac} = 275 V/cm and U_{dc} = 135 V/cm. Represented here are the velocities at μ_{dep} of -2 (solid triangle) and

-5 $\times 10^{-19}$ $m^4 \cdot V^{-2} \cdot s^{-1}$ (solid square) which are reduced comparing to the experimental data (solid diamond), indicating less prominent dANM effect.

4. Information on Supplementary Videos

This section contains detailed information on the supplementary videos referred to in the main manuscript. In all the cases, the positive direction is either defined from top to bottom or from left to right.

Video S-1: Simulation result showing the dANM migration behavior of 5.0-μm particles at U_{dc} = 150 V/cm, U_{ac} = 450 V/cm and 0.625 Hz as resultant from the migration at the end of a driving period (at 1.52 s after release). The time step size (Δt) was 0.04 s and the video was exported from COMSOL at 5 frames/s. Virtual walls were shown at 2.5 μm around each post as used in the numerical simulation model.

The details of this video are as follows: From release to 0.76 s U_{dc} - U_{ac} = - 300 V/cm was applied and particles migrated upwards as they were transported by the EOF. In the second half driving period (0.76 s to 1.52 s), U_{dc} + U_{ac} = 600 V/cm was applied. Particles migrated downwards and then were trapped at posts due to the DEP force. Therefore, after one complete driving period, the net migration of the 5.0-μm particles was in the negative direction (upwards) while the average applied driving force was positive (downwards), demonstrating the dANM behavior.

Video S-2: Simulation result showing the normal migration behavior of 3.5-μm particles at U_{dc} = 150 V/cm, U_{ac} = 450 V/cm and 0.625 Hz as resultant from the migration at the end of a driving period (at 1.52 s after release). The Δt was 0.04 s and the video was exported at 5 frames/s. Virtual walls at 1.75 μm around each post were used in the numerical simulation model.

The details are as follows: From release to 0.76 s, U_{dc} - U_{ac} = - 300 V/cm was applied and particles migrated upwards as they were transported by the EOF. In the second half driving period (0.76 s to 1.52 s), U_{dc} + U_{ac} = 600 V/cm was applied. Particles migrated downwards and were not trapped at posts due to the much weaker DEP force not capable of inducing trapping. Therefore, after one complete driving period, both the net migration of the 3.5-μm particles and the average applied driving force were in the positive direction (downwards), demonstrating normal migration behavior.

Video S-3: Experimental result showing the dANM behavior of 4.4-μm beads and the normal behavior of 0.9-μm beads at -U_{dc} = -135 V/cm, U_{ac} = 275 V/cm and 0.1 Hz as resultant from the migration during one driving period. A video was recorded at 3.6 frames/s with an exposure time of 250 ms. A 20× objective was used as described in the main manuscript. The big hollow circles in the video were the 4.4-μm beads imaged by bright field microscopy and the small fluorescent dots were the 0.9-μm beads imaged by fluorescence.

The details are as follows: First, a potential corresponding to -U_{dc} + U_{ac} = 140 V/cm was applied and both sizes of beads migrated from left to right as they were transported by the EOF. After 5 s, -U_{dc} - U_{ac} = -410 V/cm was applied in the second half driving period. 4.4-μm beads migrated from right to left and were trapped near the posts. In contrast, 0.9-μm beads migrated from right to left transported by EOF as the weak DEP force could not trap them.

Therefore, after one complete driving period, the net migration of the 4.4-μm beads was in the positive direction (from left to right) demonstrating dANM behavior while both the net migration of the 0.9-μm beads and the average driving force were in the negative direction (from right to left) demonstrating normal migration behavior.

Video S-4: Experimental result showing the dANM behavior of mouse liver mitochondria at U_{dc1} = 20 V/cm, U_{dc2} = -30 V/cm and U_{ac} = -700 V/cm at 30 kHz as resultant from the migration during one driving period. The duration for U_{dc1} or U_{dc2} was 10 s each. A video was recorded at 4.3 frames/s with 200 ms exposure time. A 60× water-immersion objective was used as described in the main manuscript. The mitochondria sample was labeled by MitoTracker Green and was imaged by fluorescence (Ex/Em = 470/525 nm as described in the main manuscript).

The details are as follows: In the first half driving period, U_{dc1} = 20 V/cm was applied and mitochondria migrated from right to left. In the second half driving period, U_{ac} = 700 V/cm at 30 kHz and U_{dc2} = -30 V/cm were applied. Most mitochondria were trapped by the nearby posts immediately upon the application of the potentials while a few could still move from left to right. Therefore, after one complete driving period, the net migration of the majority of mitochondria was in the negative direction (from right to left) demonstrating the dANM behavior while a few mitochondria followed the average driving force in the positive direction (from left to right) showing normal behavior. It is interesting to note that mitochondria showing normal behavior appeared smaller in size, indicating the potential of separation of size-varying subpopulations of mitochondria with dANM.

REFERENCES

(1) Jones, T. B. *Electromechanics of Particles;* Cambridge University Press: New York, USA, 1995.

(2) Jones, T. B. *IEEE Eng. Med. Biol. Mag.* **2003**, *22*, 33-42.

(3) Dash, S.; Mohanty, S. *Electrophoresis* **2014**, *35*, 2656-2672.

(4) Jubery, T. Z.; Srivastava, S. K.; Dutta, P. *Electrophoresis* **2014**, *35*, 691-713.

(5) Fernandez, D. P.; Goodwin, A. R. H.; Lemmon, E. W.; Sengers, J. M. H. L.; Williams, R. C. *J. Phys. Chem. Ref. Data* **1997***, 26*, 1125-1166.

(6) Sun, G.; Chen, G.; Liu, Z.; Chen, M. *Carbon* **2010***, 48*, 1434-1440.

(7) Qi, X. -Y.; Yan, D.; Jiang, Z.; Cao, Y. -K.; Yu, Z. -Z.; Yavari, F.; Koratkar, N. *ACS Appl. Mater. Interfaces* **2011***, 3*, 3130-3133.